1982

E1-E1 damping interference in the electric field quenching of spin-polarized He+2s12 ions

A. Van Wijngaarden

R. Helbing

J. Patel

Gordon W. F. Drake
University of Windsor

$E1$-$E1$ damping interference in the electric field quenching of spin-polarized He^+ $2s_{1/2}$ ions

A. van Wijngaarden, R. Helbing, J. Patel, and G. W. F. Drake
Department of Physics, University of Windsor, Windsor, Ontario, Canada N9B 3P4
(Received 8 September 1981)

When a beam of spin-polarized metastable He^+ $2s_{1/2}$ ions is quenched by an electric field $\vec{E}$, the emitted radiation intensity contains an asymmetry term proportional to $(\hat{k}\cdot\hat{E})$ $(\vec{P}\cdot\hat{k}\times\hat{E})$ where $\vec{P}$ is the spin-polarization vector and $\hat{k}$ is the direction of observation. The resulting asymmetry is nearly proportional to the level width of the $2p_{1/2}$ state in He^+. The experiment provides the first observation of the asymmetry. The measured asymmetry is $(0.007\,69\pm0.000\,10)$ in agreement with the theoretical value 0.007 618 and corresponds to a lifetime $\tau_{2p}=(0.988\pm0.013)\times10^{-10}$ sec.

I. INTRODUCTION

The angular distribution of Ly-α radiation produced by the electric field quenching of a spin-polarized beam of hydrogenic $2s_{1/2}$ ions displays a rich diversity of interference phenomena[1,2] arising from cross terms between both alternative radiation multipoles and alternative intermediate states. The dominant field-induced decay mechanism is electric dipole ($E1$) transitions to the ground state via either the $2p_{1/2}$ or $2p_{3/2}$ intermediate states. In addition, spontaneous magnetic dipole ($M1$) and induced magnetic quadrupole ($M2$) transitions are possible. We have previously investigated the $E1$-$M1$ interference effects in He^+.[1] In the present paper, we study an $E1$-$E1$ interference term which is in addition proportional (approximately) to the decay rate Γ of the $2p$ intermediate states. The result yields an accurate value for Γ.

Detailed expressions have been derived by Hillery and Mohr,[2] and by van Wijngaarden and Drake[1] for the angular and polarization dependence of the Stark induced Ly-α quench radiation. If the radiation is observed with photon-polarization insensitive detectors, and small $M2$ correction terms are omitted, then the expression for the emitted intensity in an arbitrary direction $\hat{k}$ of observation simplifies to

$$I_{\hat{k}}=\frac{\alpha k}{4\pi}[\,I_0-3\,\mathrm{Im}(V_{1/2}^{*}V_{3/2})\hat{k}\cdot\hat{E}(\vec{P}\cdot\hat{k}\times\hat{E}) +2\overline{M}\,\mathrm{Re}(V_{1/2}+V_{3/2}/2)(\vec{P}\cdot\hat{k}\times\hat{E}) +2\overline{M}\,\mathrm{Im}(V_{1/2}-V_{3/2})\hat{k}\cdot\hat{E}]\,, \tag{1.1}$$

and

$$I_0=\tfrac{1}{2}\,|\,V_{1/2}+2V_{3/2}\,|^2[1-(\hat{k}\cdot\hat{E})^2] +\tfrac{1}{2}\,|\,V_{1/2}-V_{3/2}\,|^2[1+(\hat{k}\cdot\hat{E})^2]+\overline{M}^2\,. \tag{1.2}$$

Here $\vec{P}$ is the spin-polarization vector of the ion beam and $\hat{E}$ is the direction of the applied (static) electric field $|\,\vec{E}\,|$. The V coefficients are proportional to $|\,\vec{E}\,|$:

$$V_j=\left|\frac{\vec{E}}{3}\right|\frac{\langle 1s\,|\,z\,|\,2p\rangle\langle 2p\,|\,z\,|\,2s\rangle}{E(2s_{1/2})-E(2p_j)+i\Gamma/2},\quad j=\tfrac{1}{2},\tfrac{3}{2} \tag{1.3}$$

and

$$\overline{M}=\langle 1s\,|\,M\,|\,2s\rangle$$

is the matrix element for the magnetic dipole operator.[1] The first two terms in I_0 are the dominant electric field quenching terms while the last one gives a very small contribution from magnetic dipole radiation, which may be ignored. The various terms in Eq. (1.1) are written in order of decreasing magnitude. Since the second term depends on the imaginary part of the V coefficients, it is proportional to the finite level width Γ of the $2p$ state. It will be referred to as the $E1$-$E1$ damping term. This interference effect was first derived by Hillery and Mohr.[2] The purpose of this paper is to report the first measurement of the effect.

The significance of the remaining terms in (1.1) is as follows. The $E1$-$M1$ term

$$2\overline{M}\,\mathrm{Re}[\,V_{1/2}+V_{3/2}/2](\vec{P}\cdot\hat{k}\times\hat{E})\,,$$

which was studied in detail in Ref. 1, describes interference between magnetic dipole radiation and field induced electric dipole radiation in a spontaneous transition from the $2s_{1/2}$ state to the $1s_{1/2}$ ground state. Since the last term contains the imaginary part of the $2s_{1/2}$-$2p_{1/2}$ transition energy in place of the real part, it is an order of magnitude smaller than the above $E1$-$M1$ term.

In Sec. II of the paper we study the angular dependence of the radiation for the various terms in Eq. (1.1). The experimental method is described in Sec. III and the results are presented in Sec. IV.

II. ANGULAR DEPENDENCE OF RADIATION

Since the intensities for the various angular distributions in Eq. (1.1) overlap spatially, experimental care is required to isolate the effects from the $E1$-$E1$ damping interference under investigation. To appreciate the resulting experimental procedures, we show polar diagrams for the important radiation intensities in Figs. 1(a) and 1(b). Here the He^+ $2s_{1/2}$ beam travels into the plane of the paper with a spin-polarization vector $\vec{P}=\hat{z}$, ($m_s=+\frac{1}{2}$) parallel to the beam velocity. An external electric field $\vec{E}$ makes angles of 135° or 45° with respect to the x direction in Figs. 1(a) and 1(b), respectively. The polar angle θ is the angle between $\hat{E}$ and an arbitrary observation direction $\hat{k}$. In practice (Sec. III) two photon counters view the radiation simultaneously; one from a position on the positive x axis and the other from a position on the positive y axis.

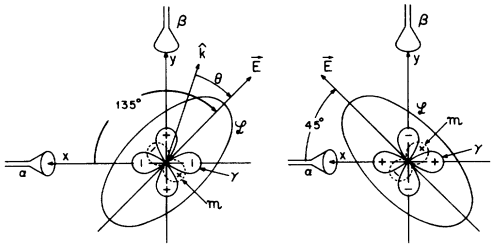

FIG. 1. Polar diagrams for two electric field directions of the three main contributions (not to scale) to the quench radiation for a spin-polarized He^+ $2s$ beam traveling along the positive z axis ($\hat{z}=\hat{x}\times\hat{y}$). In arbitrary intensity units, the distributions $\mathscr{L}=1+0.267\cos^2\theta$, $\gamma=8.6\times10^{-3}\cos\theta\sin\theta$, and $\mathscr{M}=0.0136\sin\theta\,/(|\vec{E}|\,(\mathrm{V/cm})$ represent the main quench radiation, the $E1$-$E1$ damping interference, and the $E1$-$M1$ interference distributions, respectively. α and β are the photon counters in Fig. 2.

The electric field quenching terms in I_0 [Eq. (2.1)] can be combined[3] in the form

$$\mathscr{L}(\theta)=1+\left[\left[\frac{1+R}{1-3R}-1\right]\Big/\left[\frac{1+R}{1-3R}+1\right]\right]\times\cos^2\theta\,, \tag{2.1}$$

where

$$R=\frac{\mathscr{L}(0)-\mathscr{L}(\pi/2)}{\mathscr{L}(0)+\mathscr{L}(\pi)2} \tag{2.2}$$

is the anisotropy in the electric dipole quench radiation parallel ($\theta=0$) and perpendicular ($\theta=\pi/2$) to the electric field direction. For He^+, $R=0.118$, (Ref. 4) and Eq. (2.1) becomes

$$\mathscr{L}=1+0.267\cos^2\theta\,, \tag{2.3}$$

which represents the $\mathscr{L}$ distribution in Fig. 1. Relative to the intensity of the $\mathscr{L}$ distribution, the $E1$-$E1$ damping interference can be written as

$$\gamma=8.6\times10^{-3}\cos\theta\sin\theta\,, \tag{2.4}$$

which yields the "clover leaf" distribution shown in Fig. 1. Similarly, the $E1$-$M1$ interference becomes[1]

$$\mathscr{M}=\frac{0.011\,36}{|\vec{E}|\,(\mathrm{V/cm})}\sin\theta\,, \tag{2.5}$$

which for our operating field strength of 144 V/cm is

$$\mathscr{M}=9.4\times10^{-5}\sin\theta\,, \tag{2.6}$$

The last term in Eq. (1.1) has a $\cos\theta$ dependence. It is an order of magnitude smaller than $\mathscr{M}$ and its distribution is not shown.

A comparison of Figs. 1(a) and 1(b) indicates that a rotation of the electric field through $\pi/2$ merely rotates the polar diagram through the same angle, without affecting the relative signs of the distributions. A reversal of the electric field direction, however, changes the signs of the $E1$-$M1$ interference, but not that for the $E1$-$E1$ damping interference and the $\mathscr{L}$ distribution. Hence, when the radiation intensity in an arbitrary observation direction $\hat{k}$ is averaged over two opposite electric field directions, the result does not contain contributions from the $E1$-$M1$ term. Equation (1.1) for the intensity, averaged over two opposite electric field directions, then becomes

$$\bar{I}(\hat{k}) = I_0(\hat{k}) - 3\,\mathrm{Im}(V^*_{1/2}V_{3/2})\hat{k}\cdot\hat{E}(\vec{P}\cdot\hat{k}\times\hat{E}) . \quad (2.7)$$

A. $E1$-$E1$ damping interference

From Fig. 1(a) it is apparent that the $E1$-$E1$ damping interference adds to the total intensity in the positive y direction, but subtracts from it in the positive x direction. For the field configuration shown in this figure we define the resulting $(\pi/4)-(3\pi/4)$ asymmetry as

$$A = \frac{\bar{I}(\pi/4)-\bar{I}(3\pi/4)}{\bar{I}(\pi/4)+\bar{I}(3\pi/4)} , \quad (2.8)$$

where the $\bar{I}$s are field-reversed average intensities. Substituting Eq. (2.7) with $\vec{P}=\hat{z}$ into the previous equation, and neglecting the very small $\bar{M}^2$ term in I_0, yields

$$A = B/I_0(\pi/4) , \quad (2.9)$$

where

$$B = -3\,\mathrm{Im}(V^*_{1/2}V_{3/2}) , \quad (2.10)$$

and

$$I_0(\pi/4) = 2\,|V_{1/2}|^2 - \mathrm{Re}(V_{1/2}V^*_{3/2}) + 7\,|V_{3/2}|^2/2 . \quad (2.11)$$

With the definition of the V coefficients [Eq. (1.3)] and the notation

$$\Delta_j = E(2s_{1/2}) - E(2p_j), \quad j = \tfrac{1}{2}, \tfrac{3}{2}$$

one obtains

$$A = \frac{6\Gamma/2[E(2p_{3/2})-E(2p_{1/2})]}{4\Delta^2_{3/2}-2\Delta_{1/2}\Delta_{3/2}+7\Delta^2_{1/2}+9\Gamma^2/4} , \quad (2.12)$$

which is independent of the electric field strength. Substitution of the data from Table I gives

$$A_{\mathrm{theor}} = 0.007\,618 . \quad (2.13)$$

A is related to the experimentally determined intensity ratio $r = \bar{I}(\pi/4)/\bar{I}(3\pi/4)$ by

$$A = \frac{r-1}{r+1} . \quad (2.14)$$

The corresponding theoretical value of r is

$$r_{\mathrm{theor}} = 1.01\,535 . \quad (2.15)$$

TABLE I. Input data for the calculations of the He^+ decay rate interference asymmetry.

$E(2s_{1/2})-E(2p_{1/2})$	14 042.05 MHz
$E(2p_{3/2})-E(2p_{1/2})$	175 594.0 MHz
$\Gamma(2p)$	1.002×10^{-10} sec^{-1}

III. EXPERIMENTAL

A. Overall plan

The apparatus shown in Fig. 2 is similar to that in our previous experiments.[1,3] Briefly, a 110 keV He^+ ion beam emerges from a gas cell with a few percent of metastable He^+ $2s_{1/2}$ ions in an equal statistical mixture of $m_s = +\frac{1}{2}$ and $m_s = -\frac{1}{2}$ states. The beam then enters a spin polarizer consisting of an axial magnetic field and transverse electric fields. At our field strengths of $E = 500$ V/cm, $B = 6800$ G, and with an interaction time of 2.3×10^{-8} sec, the $m_s = -\frac{1}{2}$ population is reduced by a theoretical factor of 3×10^{-12}, while the $m_s = +\frac{1}{2}$ population is reduced by only about 10% (see Ref. 1 for further details). The expected ratios were checked by monitoring the decrease in quenching signal when the spin-polarizer fields are switched on. Thus the beam leaving the spin polarizer is essentially 100% spin polarized with a spin-polarization vector $\vec{P} = +\hat{v}$ parallel to the beam velocity. Next the beam passes a prequencher consisting of cylindrical electrodes which can provide sufficiently strong axial electric fields to destroy nearly all of the metastable He^+2s ions. The prequencher potentials are only switched on for purposes of noise determinations. After the beam is collimated by circular slits of 0.15 cm diam, it passes a quenching cell consisting of four metal rods mounted on insulators in a quadrupole arrangement, and finally it enters a Faraday cup where the beam current is typically 7 μA.

To prevent disorientation of the spin directions along their flight path by Larmor precession about stray magnetic fields, the components of the magnetic field perpendicular to the beam direction are canceled with Helmholtz coils and, to ensure a sharp definition of the z axis, a relatively strong magnetic field of 20 G is applied parallel to the beam direction over the region of the quenching cell.

A static electric field which always makes an angle of either $\pi/4$ or $3\pi/4$ with one of the observa-

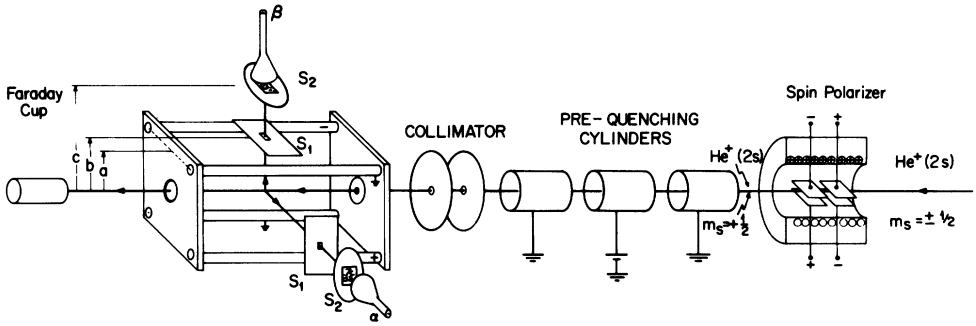

FIG. 2. Diagram of the apparatus. The dimensions shown are (a) = 1.616 cm, (b) = 4.83 cm, and (c) = 13.40 cm. The slits S_1 and S_2 are 0.737 cm$\times$0.381 cm and 0.559 cm diam.

tion axis (Fig. 1) is obtained by grounding two of the diagonally located opposite quadrupole rods and by applying opposite polarities to the other two.

B. Photon detection

The static electric field on the beam of metastables induces the emission of Ly-α (304 Å) photons. The resulting quench radiation emitted in two perpendicular directions is counted simultaneously by a double-photon counting system consisting of two channeltrons α and β which, respectively, view the radiation in the x and y directions. Counting times are normalized to a preset beam flux with the aid of the Faraday cup current. The rectangular slit S_1 (0.737 cm$\times$0.381 cm) and the circular slit S_2 (0.559 cm diam) of the photon collimators define the solid angle for observation. Slits S_1 and S_2 are mounted at a distance of 4.83 and 13.40 cm from the beam axis. Slits S_2 are covered with thin aluminum foils which are almost completely transparent to the Ly-α radiation but stop the low-energy particles that are formed by the interaction of the fast ion beam with the remaining low-pressure (5×10^{-8} Torr) gas in the quenching cell. The films reduce the noise counts by an order of magnitude and at the low quenching field $E=144$ V/cm used, the signal-to-noise ratio was as high as 25:1.

C. Intensity ratios

The ratio of the field reversed average intensities emitted along the positive and negative lobes (Fig. 1) for the damping interference distribution was measured as follows. First, for the electric field configuration of Fig. 1(a), the signal output counts S'_α and S'_β for the α and β counters are measured simultaneously. Next the electric field is reversed to obtain output counts S''_α and S''_β. The field-reversed average signal for the α counter is

$$(S_\alpha)_1=\frac{S'_\alpha+S''_\alpha}{2} .$$

This signal is given [see Eq. (2.7)] by

$$(S_\alpha)_1=\alpha[I_0(\pi/4)-PB/2] . \tag{3.1}$$

Here, $P=|\vec{\mathrm{P}}|$, and the constant α contains the solid angle and the (unknown) efficiency for photon detection. Similarly,

$$(S_\beta)_1=\beta[I_0(\pi/4)+PB/2] \tag{3.2}$$

is the field-reversed average intensity for the β counter. Finally, the field is rotated by $\pi/2$ to the configuration shown in Fig. 1(b). The field-reversed average signals now become

$$(S_\alpha)_2=\alpha[I_0(\pi/4)+PB/2] \tag{3.3}$$

and

$$(S_\beta)_2=\beta[I_0(\pi/4)-PB/2] . \tag{3.4}$$

Combining Eq. (3.1) through Eq. (3.4) yields

$$\left[\frac{(S_\beta)_1}{(S_\alpha)_1}\frac{(S_\alpha)_2}{(S_\beta)_2}\right]^{1/2}=\frac{I_0(\pi/4)+PB/2}{I_0(\pi/4)-PB/2} . \tag{3.5}$$

The left side of this equation is an experimentally determined quantity for the observed ratio $r_0=\bar{I}(\pi/4)\bar{I}(3\pi/4)$ which is independent of the efficiencies α and β of the photon detectors. It must still be corrected for noise counts, which we define

as the signal still observed after the metastable $He^+ 2s_{1/2}$ ions in the beam have been destroyed in the prequencher, and instrumental asymmetries.

D. Instrumental asymmetry effects

Since the measurement of r_0 only involves field-reversed averages of intensity ratios [Eq. (3.5)], systematic errors arising from beam current fluctuations and deflections (5×10^{-3} cm) of the ion beam by the electric quenching field $E=144$ V/cm in the observation region are automatically eliminated. However, large systematic errors can arise from the relatively large electric field quench radiation term $\mathscr{L}(\theta)=1+0.267\cos^2\theta$ if the counters are not set at exactly 45° and 135° with respect to the electric field direction. The nominal asymmetry

$$\frac{\mathscr{L}(\pi/4)-\mathscr{L}(3\pi/4}{\mathscr{L}(\pi/4)+\mathscr{L}(3\pi/4)}$$

from this term vanishes exactly. But if, for example, the α counter angle is in error by ϵ radians, then $\mathscr{L}(\theta)$ contributes an asymmetry of

$$\frac{\mathscr{L}(\pi/4-\epsilon)-\mathscr{L}(3\pi/4)}{\mathscr{L}(\pi/4-\epsilon)+\mathscr{L}(3\pi/4)}\simeq 0.17\epsilon\ . \tag{3.6}$$

For our estimated instrumental uncertainty of $\epsilon=9\times10^{-4}$ rad (0.05°) the above asymmetry is 0.000 15, which is not negligible compared to the $E1$-$E1$ damping asymmetry of $A_{\text{theor}}=0.007\,618$.

The correction for the above effect can be determined by measuring the ratio [Eq. (3.5)] with an unpolarized ($P=0$) $He^+ 2s_{1/2}$ beam. If the resulting intensity ratio is expressed in the form $1+\delta$, then the corrected value for the observed ratio r_0 for the $E1$-$E1$ damping interference is

$$r=r_0-\delta\ . \tag{3.7}$$

E. Measurement of instrumental asymmetry

Using an unpolarized $He^+ 2s$ ion beam the instrumental ratio, defined by Eq. (3.5) with $P=0$, was measured in eight different runs on different days. The results are shown in Table II. Each run consists of N separate measurements and each measurement contains about 200 000 photon counts. The mean and statistical error for each run were computed from

$$\bar{r}=\sum_{i=1}^{N}\frac{r_i n_i}{n_T}\ , \tag{3.8}$$

$$\sigma=\sum_{i=1}^{N}\frac{(r_i-\bar{r})^2 n_i^{1/2}}{n_T(N-1)}\ , \tag{3.9}$$

where n_i is the number of counts in the ith measurement and n_T is the total number of counts for the run. Averages over the runs were computed with a weighting factor of $1/\sigma_i^2$ where σ_i is the statistical uncertainty for the ith run. The run average is $\bar{r}_{\text{inst}}=0.99\,974\pm0.00\,016$ which corresponds to a δ value [see Eq. (3.6)]

$$\delta=-0.000\,26\pm0.000\,16\ . \tag{3.10}$$

Since $\delta<0$, its magnitude must be added to the observed ratio, r_0, for the polarized beam. (See Sec. IV.)

IV. RESULTS AND DISCUSSION

Using an $He^+ 2s_{1/2}$ ion beam with a spin-polarization vector $\mathbf{P}=\hat{v}$ parallel to the beam velocity, the damping interference ratio, defined by Eq. (3.5), was measured in 22 different runs on different days. The quenching field was 144 V/cm and at this field the combined photon counting rate was about 1000 per second. The results are

TABLE II. Experimental results for r_{inst}. N is the number of measurements for each run and n_T is the total number of photon counts recorded for each run.

Run	N	$n_T\times10^{-7}$	r_{inst}
1	46	0.90	0.999 94±0.000 72
2	100	1.94	0.999 50±0.000 51
3	100	2.11	0.999 96±0.000 43
4	110	2.30	0.999 80±0.000 40
5	100	2.28	1.000 01±0.000 45
6	100	2.06	0.999 55±0.000 42
7	110	2.20	0.999 97±0.000 43
8	100	2.08	0.999 33±0.000 42

shown in Table III. Computation of statistical averages is similar to that described in Sec. III. The final average result for r_0 becomes

$$\bar{r}_0 = 1.015\,24 \pm 0.000\,14 .$$

This result must be corrected for the instrumental asymmetry by adding

$$|\delta| = 0.000\,26 \pm 0.000\,16 .$$

Thus the final result for the $r = \bar{I}(\pi/4)/\bar{I}(3\pi/4)$ is

$$r = 1.015\,50 \pm 0.000\,21 .$$

A careful search was made for other possible corrections and these were found to be negligible. Our ratio value corresponds to a 45°—135° asymmetry of

$$A_{\text{expt}} = 0.007\,69 \pm 0.000\,10$$

in agreement with the theoretical value

$$A_{\text{theor}} = 0.007\,618 .$$

Thus this experiment provides the first detection and measurement of $E1$-$E1$ damping.

A. Lifetime

Since the A value in Eq. (2.12) is approximately proportional to the level width Γ of the $2p$ state, a measurement of the $E1$-$E1$ damping asymmetry is equivalent to a measurement of the lifetime $\tau = 1/(2\pi\Gamma)$. Solving Eq. (2.12) for Γ yields

$$(\tau_{2p})_{\text{expt}} = (0.988 \pm 0.013) \times 10^{-10} \text{ sec} .$$

The corresponding theoretical value is

$$(\tau_{2p})_{\text{theor}} = 0.9977 \times 10^{-10} \text{ sec} .$$

Our measurement is more accurate than the beam-foil result

$$\tau_{2p} = (0.98 \pm 0.05) \times 10^{-10} \text{ sec}$$

for He^+ by Lundin *et al.*,[5] but less precise than the beam-foil measurements for the lifetime of the $2p$ state in H of $(1.60 \pm 0.01) \times 10^{-9}$ sec by Chupp *et al.*[6] and of $(1.592 \pm 0.025) \times 10^{-9}$ sec by Bukow *et al.*[7] The estimated error in the latter experiment is larger because of a more careful treatment of cascade corrections.

The precision of our method for lifetime deter-

TABLE III. Experimental results for the decay rate interference ratio r_0. N is the number of measurement for each run and n_T is the total number of photon counts recorded for each run.

Run	N	$n_T \times 10^{-7}$	r_0
1	35	0.84	1.015 90 ± 0.000 86
2	40	1.27	1.015 08 ± 0.000 66
3	60	1.56	1.015 37 ± 0.000 59
4	100	2.65	1.015 14 ± 0.000 46
5	55	1.48	1.014 95 ± 0.000 54
6	50	0.99	1.015 84 ± 0.000 65
7	60	1.41	1.015 54 ± 0.000 53
8	50	1.11	1.015 70 ± 0.000 61
9	60	1.36	1.015 44 ± 0.000 62
10	60	1.30	1.015 62 ± 0.000 50
11	50	0.97	1.014 25 ± 0.000 71
12	15	0.23	1.013 71 ± 0.001 05
13	100	1.85	1.015 71 ± 0.000 56
14	60	1.09	1.015 74 ± 0.000 69
15	65	1.15	1.014 89 ± 0.000 48
16	50	0.75	1.016 20 ± 0.000 70
17	18	0.29	1.015 07 ± 0.001 71
18	25	0.50	1.014 46 ± 0.000 88
19	70	1.63	1.013 99 ± 0.000 53
20	40	1.17	1.014 97 ± 0.000 57
21	25	1.10	1.016 56 ± 0.000 73
22	40	0.98	1.014 96 ± 0.000 54

minations was hampered by the instrumental asymmetry of the apparatus. However, we have demonstrated that this asymmetry is small. It can be shown that the instrumental asymmetry can be eliminated to first order in ϵ by averaging the measurements over the two polarization vectors $\vec{P}=+\hat{v}$ and $\vec{P}=-\hat{v}$, parallel and antiparallel to the beam velocity. Thus, by collecting half of the total asymmetry measurements with $\vec{P}=+\hat{v}$ and the other half with $\vec{P}=-\hat{v}$, the resulting asymmetry, averaged over the opposite spin-polarization vectors, depends only quadratically on the instrumental asymmetry. Experiments to obtain higher precision by this method are now in progress.

[1]A. van Wijngaarden and G. W. F. Drake, Phys. Rev. A 25, 400 (1982).
[2]M. Hillery and P. J. Mohr, Phys. Rev. A 21, 24 (1980).
[3]A. van Wijngaarden and G. W. F. Drake, Phys. Rev. A 17, 1366 (1978).
[4]G. W. F. Drake, S. P. Goldman, and A. van Wijngaarden, Phys. Rev. A 20, 1299 (1979).
[5]L. Lundin, H. Oona, W. S. Bickel, and I. Martinson, Phys. Scr. 2, 213 (1970).
[6]E. L. Chupp, L. W. Dotchin, and D. J. Pegg, Phys. Rev. 175, 44 (1968).
[7]H. H. Bukow, H. V. Buttlar, D. Haas, P. H. Heckmann, H. Holl, W. Schlagheck, D. Schürmann, R. Tielert, and R. Woodruff, Nucl. Instrum. Methods 110, 89 (1973).